Marine Environmental Research 195 (2024) 106351

Contents lists available at ScienceDirect

Marine Environmental Research

journal homepage: www.elsevier.com/locate/marenvrev

The thermal journey of macroalgae: Four decades of temperature-induced changes in the southeastern Bay of Biscay

O. Arriaga [a,*], P. Wawrzynkowski [b,c], N. Muguerza [a], I. Díez [a], J.M. Gorostiaga [a], E. Quintano [a], M.A. Becerro [b]

[a] Laboratory of Botany, Department of Plant Biology and Ecology, Fac. of Science and Technology & Research Centre for Experimental Marine Biology and Biotechnology PIE-UPV/EHU, University of the Basque Country (UPV/EHU), PO Box 644, 48080, Bilbao, Spain
[b] The BITES Lab, Center for Advanced Studies of Blanes (CEAB-CSIC), Access Cala S Francesc 14, 17300, Blanes, Girona, Spain
[c] University of Girona, Institute of Aquatic Ecology, C/ Maria Aurèlia Capmany 69, Girona, E-17003, Catalonia, Spain

ARTICLE INFO

Keywords:
Global warming
Temperature
Macroalgae
Subtidal
Community Temperature Index (CTI)
Community composition
Temporal variability
Bay of Biscay

ABSTRACT

Global warming is triggering significant shifts in temperate macroalgal communities worldwide, favoring small, warm-affinity species over large canopy-forming, cold-affinity species. The Cantabrian Sea, a region acutely impacted by climate change, is also witnessing this shift. This study delved into the impacts of increasing sea surface temperature on the subtidal macroalgal communities in the southeastern Bay of Biscay over the last four decades, by using data from the years 1982, 2007, 2014, and 2020. We found that temperature has shaped the community structure, with warm-affinity species steadily displacing their cold-affinity counterparts. Notably, new communities exhibited a profusion of smaller algal species, explaining the observed increased biodiversity within the area. In the last period investigated (2014–2020), we observed a partial recovery of the communities, coinciding with cooler sea surface temperatures. Shallow algal communities were more reactive to temperature variations than deeper communities, possibly associated with higher exposure to increased temperatures. Our study offered insights into the intricate relationship between the changes in ocean temperature and algal species in the southeastern Bay of Biscay, shedding light on the ongoing ecological shifts in this region.

1. Introduction

Our planet is undergoing a troubling trend of rapid warming that is expected to persist in the near future (2021–2040; IPCC, 2023). Over 90% of this excess heat has been absorbed by the oceans, resulting in a significant 0.88 °C increase in sea surface temperature in 2010–2020 compared to the pre-industrial 1850–1900 period (IPCC, 2023). Beyond this gradual temperature rise, a surge in acute and extreme warming events (heatwaves), which have increased in frequency and duration over the past century, has also been reported (Oliver et al., 2018). In this changing context, non-mobile, temperature-sensitive organisms such as macroalgae are subjected directly to increased temperature and heatwaves (Smale, 2020). It is becoming increasingly clear that macroalgal communities are suffering the consequences of global warming over the last two decades. Worldwide, there is a transition from the dominance of canopy-forming species to the prevalence of turf-like or invasive species (Filbee-Dexter et al., 2016; Gorman et al., 2020; Perkol-Finkel and Airoldi, 2010). The take-over of warm-adapted species at the expense of their cold-adapted counterparts is a trend in the world's temperate oceans (Burrows et al., 2019; Smale and Wernberg, 2013). While environmental and anthropogenic factors like eutrophication, urbanization, extreme wave events, ocean currents, or solar radiation contribute to changes in macroalgal communities (Borja et al., 2018; Fernández, 2011; Gouvêa et al., 2017; Quintano et al., 2017), temperature rises as the main driver of these transformations (Díez et al., 2012; Tanaka et al., 2012; Verdura et al., 2021). Remarkably, temperature dictates the latitudinal distribution of macroalgal species and determines their vertical distribution (Harley et al., 2012). Consequently, as global warming unveils, species will likely venture deeper into the water column, drawn by the cooler seawater found there (Assis et al., 2017). As a compelling example from the Northern Iberian Peninsula, a subsequent recovery after a massive temperature-driven decline of a kelp forest occurred in deeper waters (Voerman et al., 2013).

The Cantabrian Sea, a narrow temperate coastal shelf sea in the

* Corresponding author.
E-mail addresses: olatz.arriaga@ehu.eus (O. Arriaga), paul.wawrzynkowski@udg.edu (P. Wawrzynkowski), nahiara.muguerza@ehu.eus (N. Muguerza), isabel.diez@ehu.eus (I. Díez), jm.gorostiaga@ehu.eus (J.M. Gorostiaga), endika.quintano@ehu.eus (E. Quintano), mikel.becerro@csic.es (M.A. Becerro).

https://doi.org/10.1016/j.marenvres.2024.106351
Received 3 October 2023; Received in revised form 7 January 2024; Accepted 9 January 2024
Available online 11 January 2024

southern Bay of Biscay along the Spanish northern coast, has a noteworthy departure from global temperature trends. Since the 80s, the sea surface temperature in this region has been increasing at a rate of 0.23 °C decade^{-1} (Chust et al., 2022), exceeding the global average of 0.15 °C decade^{-1} (Rhein et al., 2013). This warming rate intensifies towards the east, into the inner Bay of Biscay (Lavín et al., 2006). The alteration in temperature in this region also encompasses the occurrence of extreme heatwaves, with a notable increase in their frequency and duration (Izquierdo et al., 2022). In the eastern part of the Cantabrian Sea, the summers of 1997, 2003, and 2006 were exceptionally warm, with seawater temperatures surpassing 25 °C (Díez et al., 2012). This warming trend has had a discernible impact on the ecosystem, particularly affecting the canopy-forming species *Gelidium corneum*. The drastic decline of this species has been attributed to increasing wave energy (Borja et al., 2018), solar radiation (Quintano et al., 2019), temperature increase, or a synergy of these factors (Díez et al., 2012). This species used to form extensive stands, creating a complex and stable community that functioned as food, shelter, nursery, and habitat for a variety of associated organisms, from fish to invertebrates and other small algae (Borja et al., 2004; Bustamante et al., 2014). Following this decline, no other canopy-forming species has been reported to assume these critical ecological functions.

Studying the response of macroalgal communities to ocean warming is paramount for marine biodiversity conservation, given the fundamental roles they play in shallow rocky shore ecosystems. The decline of canopy-forming species within these communities can trigger a series of ripple effects throughout the entire ecosystem, exerting detrimental consequences on associated species and ultimately leading to significant economic losses. This study delved into the repercussions of escalating sea surface temperatures on macroalgal communities in the southeastern Bay of Biscay. We gathered data spanning 38 years (1982–2020) along a depth gradient. We looked at how the macroalgal communities changed over this time period and set to disentangle the influence of temperature on community shifts. Our first objective was to assess whether temperature stood as the primary driver behind the structural changes observed in the community. We computed the Community Temperature Index (CTI) to achieve this goal. This thermal metric isolates the effect of temperature on the entire community (Devictor et al., 2008), thus shedding light on the community thermal requirements and the degree to which macroalgal species meet such requirements. Our second objective was to detect potential temporal variations in CTI and community composition along the depth gradient. Lastly, our third objective was to disentangle CTI variations into four underlying processes outlined by McLean et al. (2021): tropicalization, borealization, detropicalization, and deborealization. The significance of examining these goals lies in the critical need to comprehend the mechanisms at play in macroalgal communities. We expected temperature to be a main driver of community change and hypothesized an increase in warm-affinity over cold-affinity species. We expected distinct responses from communities inhabiting shallower and deeper habitats.

2. Methods

2.1. Study area

The study area is located in the eastern Cantabrian Sea (southeastern Bay of Biscay), specifically on the western Basque Coast, between the localities of Kobaron (43°21′14″ N 03°09′14″ W) and Muskiz (43°21′18″ N 03°07′48″ W; Fig. 1). This open coastline is exposed to swells from NW, WNW and NNW (González et al., 2004). The temperature at the eastern Cantabrian Sea used to be between 12 °C in winter and 22 °C in summer (Borja et al., 2000), but since the 1980s sea surface temperature has warmed up at a rate of 0.15 and 0.25 °C decade^{-1}, mainly at the surface (Chust et al., 2022).

2.2. Field data collection

Data included four sampling surveys in the summer months (July and August) of 1982, 2007, 2014, and 2020 (Gorostiaga, 1995; Muguerza et al., 2022b). Along this 1.8 km stretch of coastline, we studied seven sites, and in each of them, we collected information at six depths below extreme low water spring tides (2 m, 3 m, 6 m, 9 m, 10 m, and 11 m). Starting at a depth of 2 m below chart datum, we studied a surface area of 2000 cm^2 (40 × 50 cm quadrats) at each depth. We laid down these quadrats in stable substrates (continuous bedrock) with slight to moderate slopes (<30°), following a north-south orientation (perpendicular to the coastline) and avoiding habitats such as crevices or boulders.

We collected all the flora within the delimited surface except for the calcareous crustose layer. These samples were transferred to the laboratory and kept frozen in labeled plastic bags. To analyze the samples, we unfrozen them, separated them by species, and identified all species following the taxonomic nomenclature used in AlgaeBase (Guiry and Guiry, 2023). We then calculated the dry weight (in grams) of each identified species (100-110 °C, 24 h).

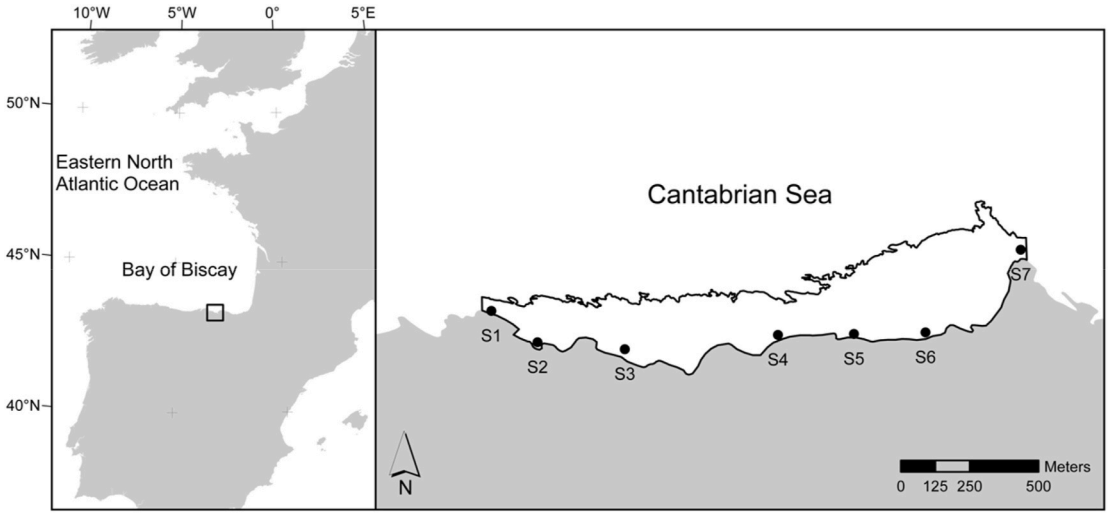

Fig. 1. Map of the study area with the seven sites (S). The section refers to the studied area (limit W-E), and the delimitation of the maximum depth sampled (11 m). Bathymetry obtained from Eusko Jaurlaritza/Gobierno Vasco.

2.3. Occurrence records and temperature data collection

We calculated the thermal optimum of each species (Species Temperature Index, STI) as the mean range of the maximum and the minimum temperature at which the species occur (Devictor et al., 2012). We also calculated the thermal requirement of the community using the Community Temperature Index (CTI), a measure of the average thermal affinity of ecological communities. The CTI is the abundance-weighted STI average of all species in a sampling unit (Devictor et al., 2008, 2012). Thus, for this study, we calculated CTI using the biomass-weighted STI average of the species.

We obtained species distribution data from the global open-access databases "Ocean Biodiversity Information System" (OBIS) (https://www.obis.org/) and "Global Biodiversity Information Facility" (GBIF) (https://www.gbif.org/) by using the special packages robis (Provoost and Bosch, 2019) and rgbif (Chamberlain et al., 2021) from the open-source software R (RStudio Team, 2016). The time frame considered for occurrence records was 1993–2020. Out of the 129 species identified, six species were not included in the analyses due to a lack of distributional information.

We downloaded monthly SST data from the E.U. Copernicus Marine Service Information, specifically from the Multi Observation Global Ocean 3D Temperature Salinity Height Geostrophic Current and MLD dataset (https://doi.org/10.48670/moi-00052).

2.4. Data treatment

We calculated the mean annual SST to construct a time series (1982–2020) to study the SST evolution.

With the biological data, we first performed univariate analyses of CTI, total biomass, Shannon diversity Index, and species richness to test for temporal changes. To test for homogeneity of dispersion, we ran a permutational analysis of multivariate dispersions (PERMDISP) test using PERMANOVA + for PRIMER software (Anderson et al., 2008). We also performed PERMANOVA analyses with two factors, time (random) and depth (fixed), and *post-hoc* pairwise comparisons using Gosset's t statistic to test for differences within factors (Anderson et al., 2008). We favored PERMANOVA over parametric ANOVA due to its ability to handle non-normal data effectively, making it more suitable when data fail to meet parametric assumptions, as in our study. When there was a significant interaction between the factors, we visually represented the temporal evolution of the variables at each depth. We compared the differences (distances) between these depths for that particular variable at the end (2020) of the study.

We studied the correlation between temporal SST changes and the temporal changes in the mean CTI values at 2 and 3 m depth, given that we did not have *in situ* temperature measurements for each depth and that satellite-based SST values would fit better the actual values of these shallow depths. Considering the small sample size, we also cross-validated this correlation with a bootstrapping method.

We performed multivariate analyses to detect spatio-temporal changes in the community structure using PERMANOVA + for PRIMER software (Anderson et al., 2008). Biomass data was previously square root transformed to reduce the influence of the most dominant taxa and let species with intermediate abundance play a part. We constructed a resemblance matrix based on Bray-Curtis similarities and performed a non-metric multidimensional scaling diagram (nMDS) to visually assess the similarity of the communities at different depths and years. We followed the same PERMANOVA procedure explained above to assess the influence of time and depth in the communities. We also compared the differences in the distances between communities at different depths at the end (2020) of the study.

We performed a similarity percentage analysis (SIMPER) to know which species were responsible for the differences between the communities in 1982 and 2020. We created two groups with those species contributing >1% to the dissimilarity, based on their biomass evolution. The species that increased their biomass during the study period were assigned to the "increase" group, and those that decreased biomass to the "decrease" group. We then represented the temporal evolution of their biomass, and performed a PERMDISP analysis, a PERMANOVA analysis, and pairwise comparisons following the same procedure mentioned earlier. We calculated the mean thermal optimum of each group. We used a single factor ANOVA to test for significant differences since data followed a normal distribution and both groups had equal variances.

The changes in the mean thermal affinity (CTI) of a community can be decomposed into four processes (McLean et al., 2021: Fig. 2). An increase in the CTI is always due to the larger relative abundance of warm-affinity species, which could respond to the rise of warm-affinity species (tropicalization) or the reduction of cold-affinity species (deborealization). Similarly, a decrease in the CTI is necessarily linked to a larger relative abundance of cold-affinity species, which could respond to the reduction of warm-affinity species (detropicalization) or the rise of cold-affinity ones (borealization). Therefore, increases in CTI occur when the combination of tropicalization and deborealization is larger than the combination of detropicalization and borealization. Following McLean et al. (2021), we used these four processes to decompose the CTI changes at each of the three time periods (1982–2007; 2007–2014; 2014–2020). We illustrated the contribution of each process considering all depths together and also separating shallow-intermediate (2–9 m) and deep (10–11 m) communities. Warm-affinity species are those whose thermal optimum is higher than the mean CTI, and cold-affinity species are those whose thermal optimum is below the mean CTI. To assess the accuracy of this approach, we correlated the value of (tropicalization + deborealization) – (detropicalization + borealization) to changes in CTI (McLean et al., 2021).

Finally, we plotted the temporal evolution of the main canopy-forming species that declined (*Gelidium corneum*) and increased (*Gongolaria baccata*), considering shallow-intermediate and deep depths.

3. Results

We detected an increasing trend of the satellite-based sea surface temperature annual data ($p < 0.001$) for the period 1982–2020 (Fig. 3). In 1982, the mean SST was 16.11 °C, and in 2020, SST increased up to 16.97 °C (0.86 °C warmer).

We found a significant variation in the dispersion of the data for CTI, Shannon diversity index, and species richness, but not for biomass (Appendix A).

The mean Community Temperature Index increased from 12.39 ±

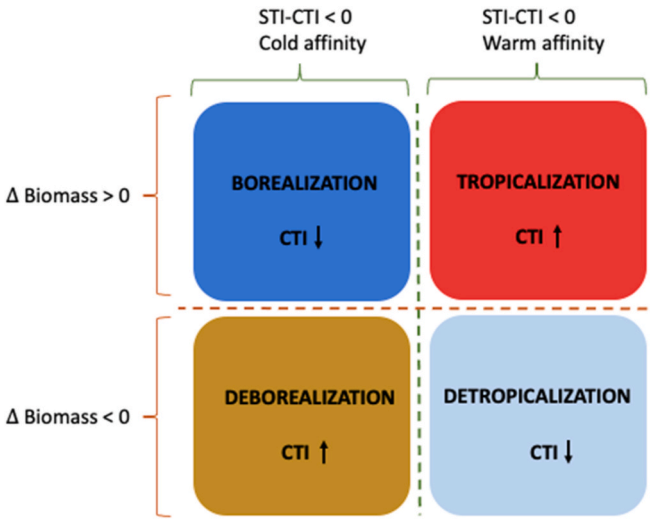

Fig. 2. The four underlying processes contributing to changes in CTI. Source: modified from McLean et al. (2021).

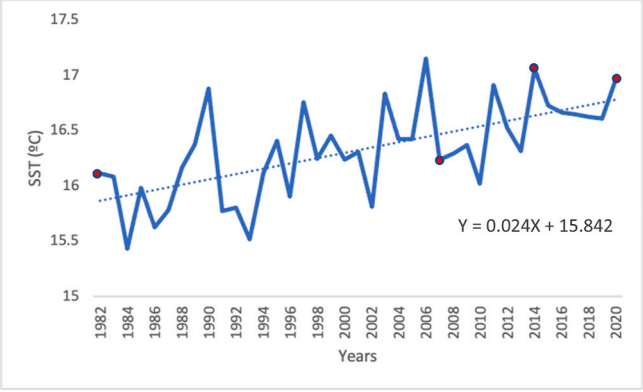

Fig. 3. Time series of Sea Surface Temperature (SST) annual data from 1982 to 2020. Red dots show SSTs of sampling years.

0.09 °C (mean ± SE) in 1982 to 13.17 ± 0.27 °C in 2007 and to 13.85 ± 0.36 °C in 2014, but then decreased slightly to 13.48 ± 0.26 °C in 2020 (Fig. 5a). The temporal evolution of the CTI varied with depth. At shallow and intermediate depths (2–9 m), mean CTI values were different at the beginning (1982) and the end (2020) of the study. In the particular case of 3 m depth, the mean CTI value of 1982 differed from the mean values of each of the other three years. We found no temporal changes at deep depths ($p = 0.021$, Appendix B.1).

Temporal CTI variation from shallow communities (2 and 3 m) positively correlated with temporal SST variation (Fig. 4), although it failed within bootstrap-generated 95 confidence intervals (CI: 0.455, 1.000).

We found no significant differences in the temporal evolution of the mean total biomass (Fig. 5b, $p = 0.353$, Appendix B.2). Shannon diversity index increased over the study period (Fig. 5c) regardless depth ($p < 0.001$, Appendix B.3). Mean species richness increased in 2007 and 2020 compared to 1982 (Fig. 5d) regardless depth ($p < 0.001$, Appendix B.4).

We differentiated two groups of species according to whether their biomass increased or decreased over time (Appendix C). We found no difference in the dispersion of the data ($p > 0.05$). The group "decrease" (Fig. 6, left), formed by six species (Appendix C), declined sharply from 1982 to 2007 and moderately from 2007 to 2014. From 2014 to 2020 the changes were not statistically significant (Appendix D). The "increase" group (Fig. 6, left), formed by 20 species (Appendix C), increased its biomass from 1982 to 2020, but the differences between the three last years were not statistically significant (Appendix D). The differences between the groups were statistically different in each year except for 2007 (Appendix D).

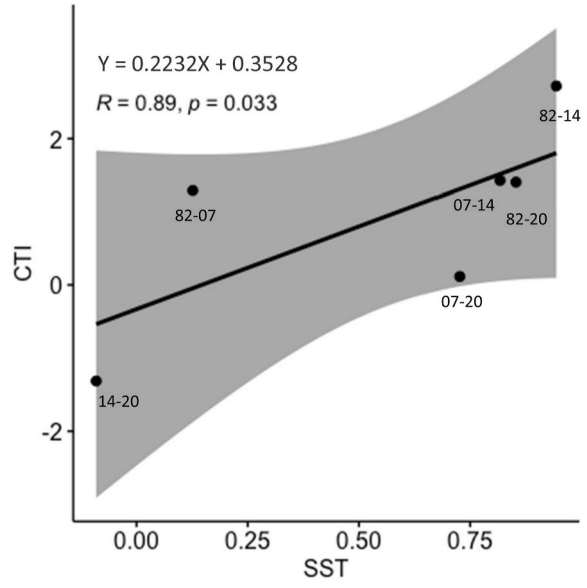

Fig. 4. Association between temporal changes in annual SST and changes in mean CTI of shallow depths (2 and 3 m).

The thermal optimum of the group "increase" was significantly higher ($p = 0.047$, Appendix E) than that of the group "decrease", with mean values of 13.618 °C and 11.693 °C, respectively (Fig. 6, right).

The temporal variation of the CTI was different for each depth (Fig. 7; Appendix B.1). At 2, 3, and 6 m, the CTI reached its maximum in 2014, and in 2020, it decreased. CTI at 9 m closely followed the trend of 6 m, although a sharp increase from 2014 to 2020 was observed, overpassing the CTI at 6 m depth. At deeper waters (10 m and 11 m), CTI values were similar at the beginning and at the end of the study period, but at 11 m, we observed a rise in CTI (over 13 °C).

In 1982, CTI values were around 12 °C for every depth except for 2 m (around 13 °C). In 2020, CTI values for 2, 3, 6, and 9 m were over 13.5 °C, whereas for deep depths (10 m and 11 m), CTI values were below 12 °C (0.174 °C lower than in 1982). We detected significant differences ($p < 0.001$) between shallow-intermediate (2, 3, 6, 9 m) CTI values and deep (10, 11 m) CTI values in 2020.

We found three groups at a 40% similarity level (Non-metric multidimensional scaling (nMDS), Fig. 8). Group A included communities from 1982 (except 2 m) and communities at 6 m depth from 2007. Group B included deeper communities (9, 10, and 11 m from 2007; 6, 9, 10, and 11 m from 2014; 10 and 11 m from 2020), and Group C was formed by shallow communities (2 m from 1982; 2 and 3 m from 2007, 2014, and 2020) together with intermediate communities (6 and 9 m) from 2020.

We found a significant variation in the dispersion of the community structure data (Appendix F). The differences between years in the community structure differed with depth (significant Year X Depth interaction, two-way PERMANOVA, $p < 0.001$, Appendix G). We also found significant differences in community structure between shallow-intermediate (2 m, 3 m, 6 m, and 9 m) and deep (10 m and 11 m) communities for 2020 ($p = 0.006$).

In the first period investigated (1982–2007), deborealization was the primary process responsible for the increasing CTI, then tropicalization and borealization (Fig. 9, left). In the second period (2007–2014), tropicalization was the primary process responsible for the increasing CTI. In the last period (2014–2020), CTI decreased and detropicalization was the primary process responsible for the decline. We found a strong correlation ($R = 0.986$) between the value of (tropicalization + deborealization) – (borealization + detropicalization) and changes in CTI (Fig. 9, right).

The processes behind CTI changes differed between shallow-intermediate and deep communities. For the shallow-intermediate communities, CTI increased within the two first periods and decreased in the last one (Fig. 10, left). Tropicalization and deborealization had a similar impact within the first period while tropicalization and detropicalization were the primary processes in the second and third periods. We found a strong correlation ($R = 0.966$) between the value of (tropicalization + deborealization) – (borealization + detropicalization) and changes in CTI (Fig. 10, right).

In deep communities, CTI increased in the first period and decreased within the last two periods. Overall, the primary process was borealization, followed by deborealization (Fig. 11, left). We found a strong correlation ($R = 0.949$) between the value of (tropicalization + deborealization) – (borealization + detropicalization) and changes in CTI.

The species *Gelidium corneum*, from the "decrease" group, declined primarily in the shallow-intermediate communities. The species *Gongolaria baccata*, from the "increase" group, primarily increased in the deep communities (Fig. 12).

4. Discussion

Our study investigated the response of macroalgal communities to nearly four decades of increasing sea surface temperature while also examining the influence of depth. By analyzing the evolution of the

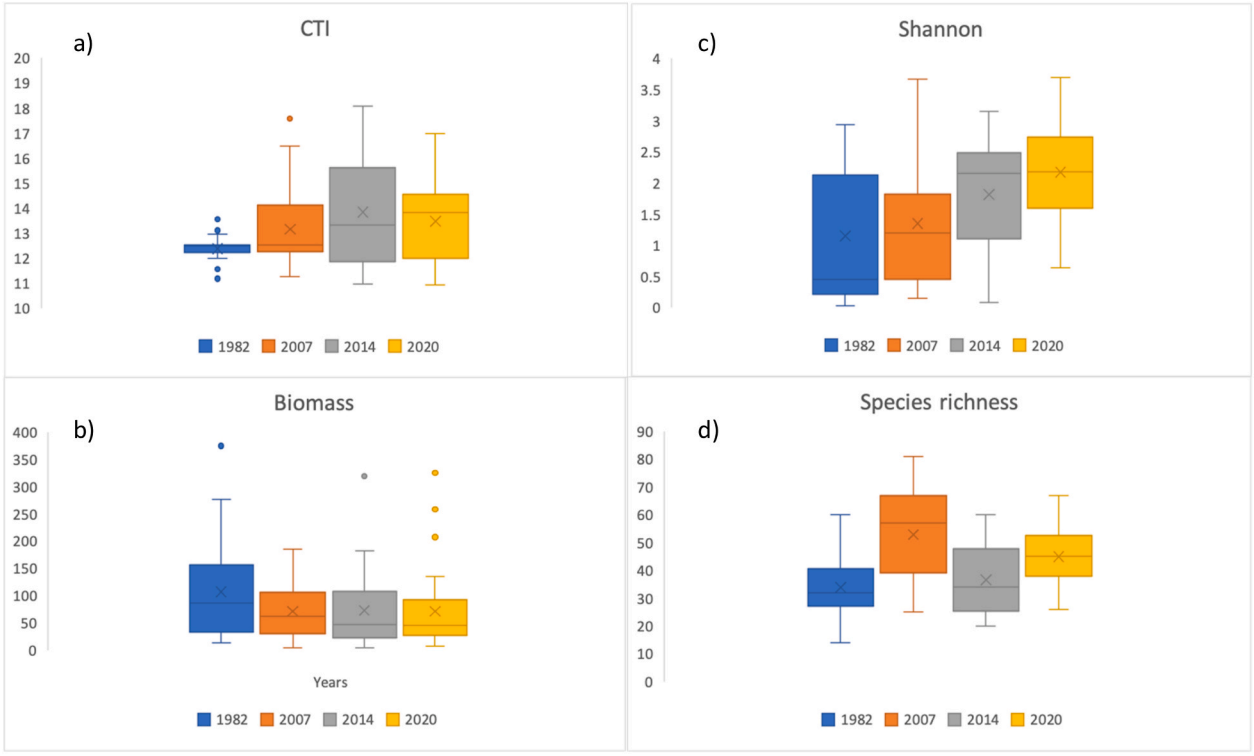

Fig. 5. Temporal evolution of a) mean annual CTI (°C), b) total biomass (g DW * 2000 cm^{-2}), c) Shannon diversity, d) Species richness, and the standard error. The line inside the box refers to the median and the X to the mean.

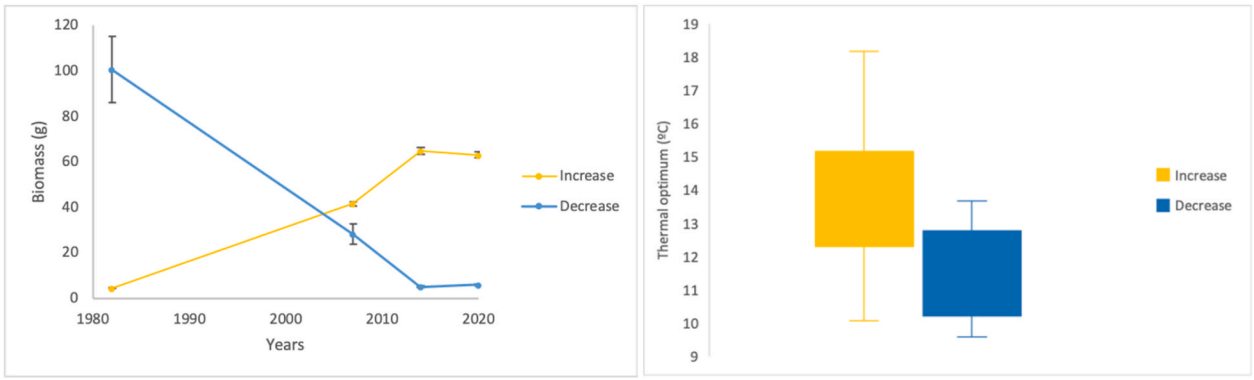

Fig. 6. Left: Mean biomass (g DW · 2000 cm^{-2}) variation along the years covered in the study for each group and the standard error. Right: mean thermal optimum of each group and the standard error.

Community Temperature Index (CTI) and community structure, we observed that warming-induced changes occurred at shallow and intermediate (2–9 m) depths but not at deep depths (10–11 m), although the community structure did change at deep depths. Cold-affinity species were progressively replaced by warm-affinity species comprising numerous but small-sized turf and coralline species, resulting in increased diversity. Changes in dispersion over the years, especially when compared to 1982, suggested a decline in the community's homogeneity. This decline is likely due to the varied evolution occurring at multiple depths. Shallow communities underwent significant structural changes in the four decades investigated, while deep communities remained relatively stable. As a result, these dynamics led to a higher community dispersion at the end of the study period.

Across three study periods (1982–2007, 2007–2014, and 2014–2020), our findings revealed distinct CTI dynamics. The initial period (1982–2007) witnessed a CTI rise primarily linked to a decline in cold-affinity species. In the second period (2007–2014), CTI increased due to a rise in warm-affinity species. In the final period (2014–2020), coinciding with a decrease in SST, CTI declined (especially in shallow waters) due to a reduction of warm-affinity species.

These observations aligned with Muguerza et al. (2022b) findings, who reported an overall biomass loss primarily driven by the decline of the canopy-forming *Gelidium corneum* and an increase in larger species like *Gongolaria baccata*, *Halopithys incurva*, and *Codium decorticatum* between 1982 and 2014. The development of an extensive canopy structure remained incomplete in 2014. Our study extended the research timeline to include data from 2020 and established associations between the documented algal changes and sea surface temperatures, providing a comprehensive understanding of the ongoing climate-induced transformations in these macroalgal communities.

We observed a progressive increase in the thermal requirements of the community, with the year 2014 registering the highest CTI values, followed by a slight decline in 2020. Notably, 2014 featured the highest mean annual SST of the decade. In that year, CTI displayed a significant

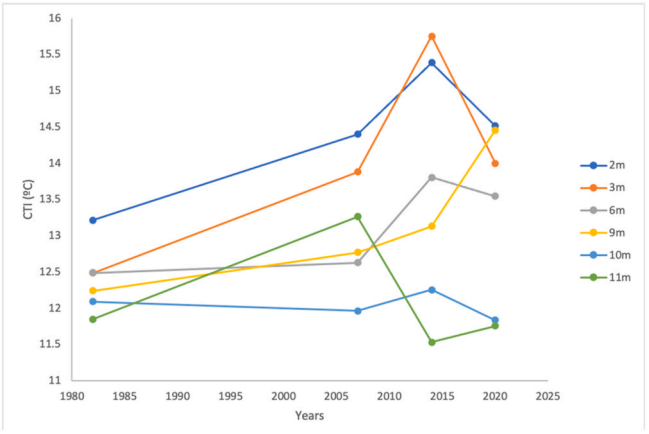

Fig. 7. Mean CTI (°C) variation along the time range considered in the study for each depth.

increase at 2 and 3 m depth, considerably surging above 15 °C and marking the peak CTI values of the study period. At depths of 6 and 9 m, CTI also increased compared to 2007, although not as pronounced as in shallower depths. Contrastingly, at depths of 10 and 11 m, CTI values remained relatively low. Seasonal dynamics, where SST rises in spring while wind intensity diminishes, reducing turbulence and enhancing water column stratification through early autumn (Valencia et al., 2004), are prone to accentuate the influence of temperature in shallow waters.

Furthermore, considering the exceptional warmth of 2014, it is plausible that surface layers experienced significant warming, with heat transferring through the water column to intermediate depths. This thermal gap likely led to forming two distinct layers with differing temperatures and densities, preventing mixing and giving rise to the observed differentiation between shallow-intermediate and deep communities. Unfortunately, *in situ* SST data for each depth was unavailable. The subsequent years, between 2015 and 2019, were progressively cooler, with a resurgence of warmth in 2020. Following the stress produced by the warm year of 2014, the subsequent five cooler years might have influenced the composition of the community observed in 2020. Many of the species observed in 2020 have life cycles exceeding a year; thus, prevailing environmental conditions could have shaped the 2020 community (Chust et al., 2022). If our interpretation is correct, our results offer some hope for the resilience of the community. In a relatively short period of cooling, the community responded by partially replacing warm-affinity with cold-affinity species, a noteworthy outcome that

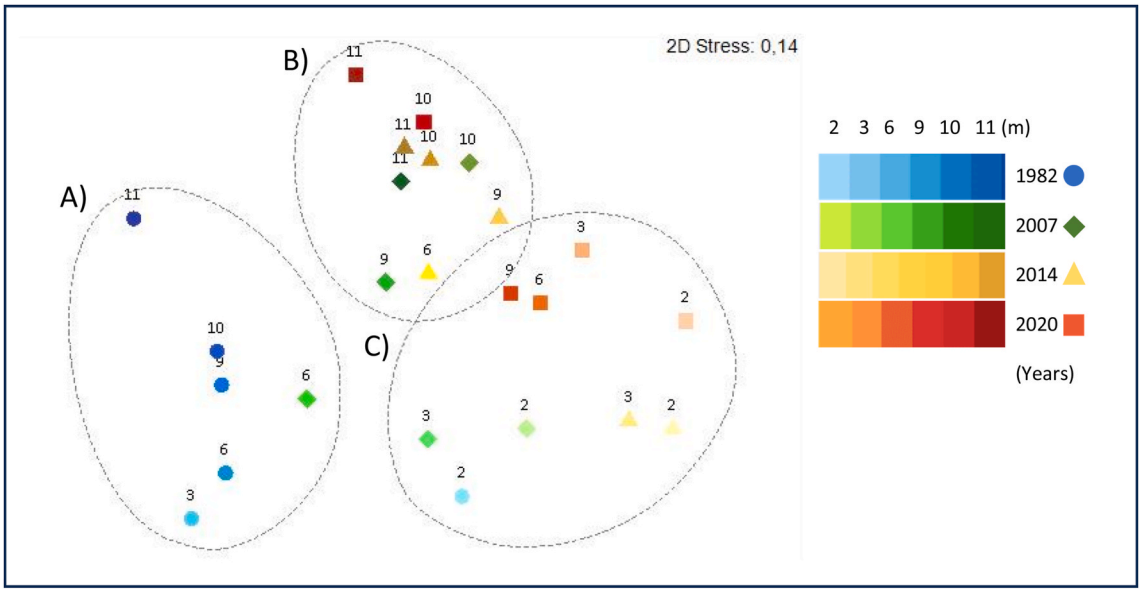

Fig. 8. Non-metric multidimensional scaling (nMDS) diagram (Anderson et al., 2008) of the mean sampling years and depths, based on Bray-Curtis similarities and square-root transformed biomass data. 40% similarity level is plotted.

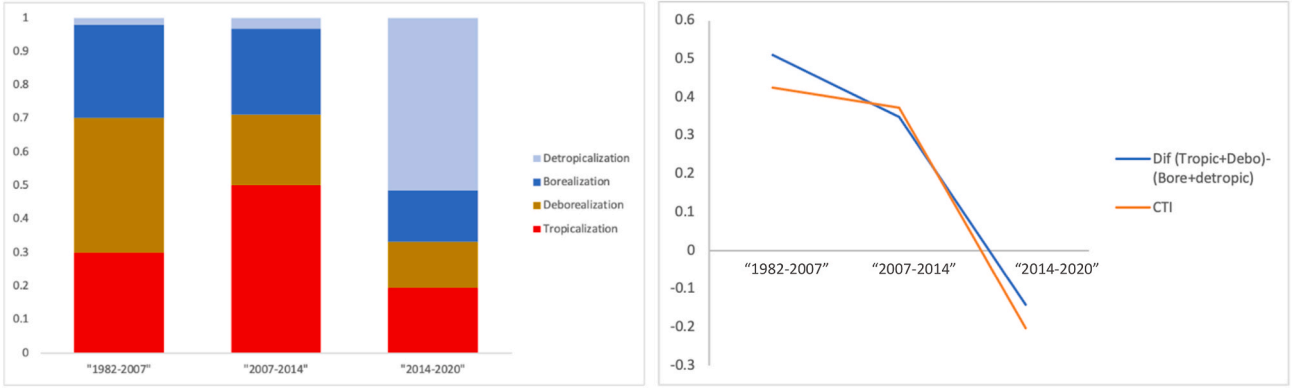

Fig. 9. Left: Contribution of each process to CTI variation for each period. Right: correlation between the value of (tropicalization + deborealization) – (borealization + detropicalization) and changes in CTI.

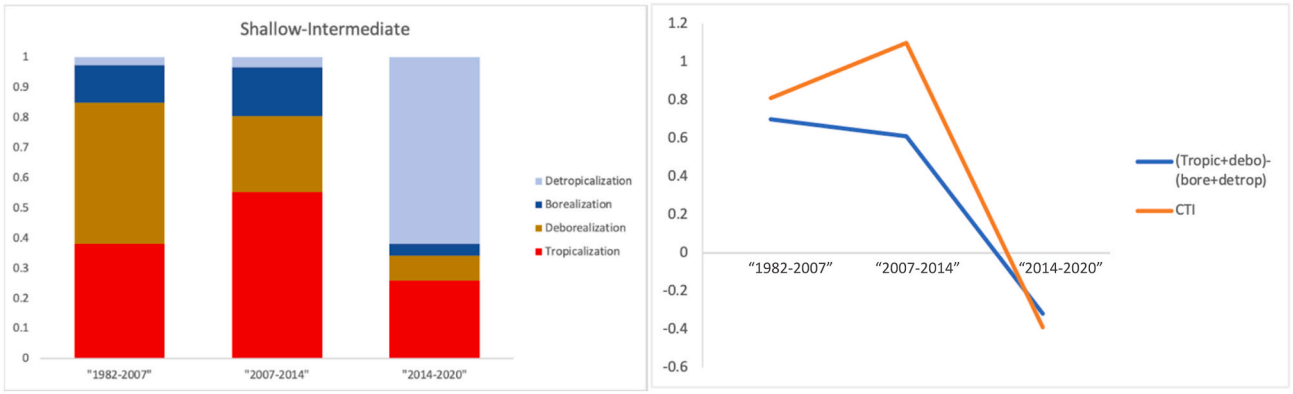

Fig. 10. Left: Contribution of each process to CTI variation for each period in shallow-intermediate communities (2 m, 3 m, 6 m, and 9 m). Right: correlation between the value of (tropicalization + deborealization) – (borealization + detropicalization) and changes in CTI.

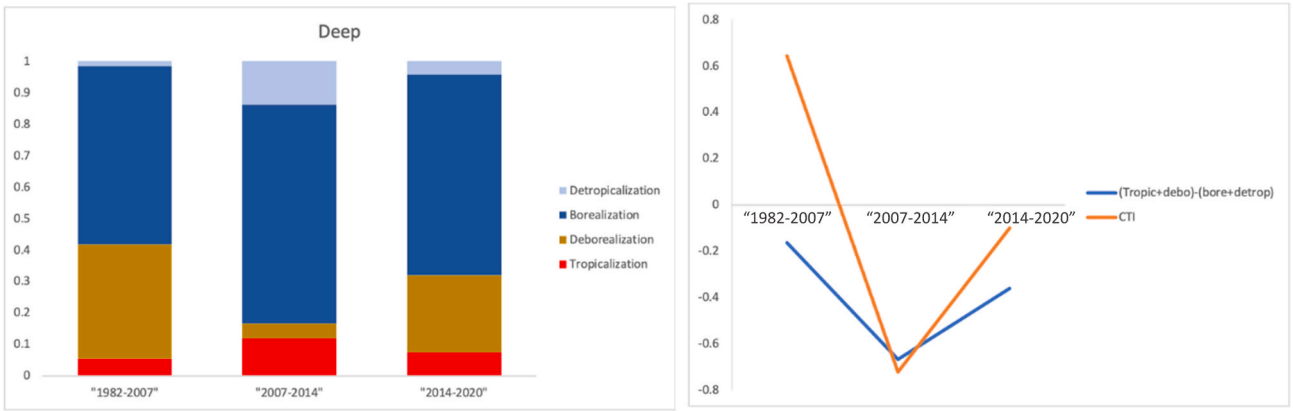

Fig. 11. Left: Contribution of each process to CTI variation for each period in deep communities (10 m and 11 m). Right: correlation between the value of (tropicalization + deborealization) – (borealization + detropicalization) and changes in CTI.

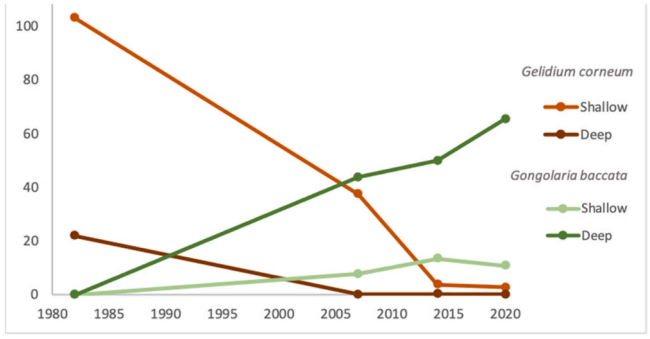

Fig. 12. Temporal variation of the biomass of Gelidium corneum and Gongolaria baccata at shallow-intermediate (2 m, 3 m, 6 m, and 9 m) and deep (10 m and 11 m) depths.

should not be overlooked. A more pronounced resilience phenomenon was also reported in another central Cantabrian locality (Lastres) due to cooling waters between 2015 and 2019 (Arriaga et al., 2023).

In 1982, the species *Gelidium corneum* formed extensive stands between 3 and 9 m depth, with their upper boundary at 2 m defined by turf vegetation comprised of *Ellisolandia elongata*, *Gelidium spinosum*, *Falkenbergia* phase of *Asparagopsis armata*. At the lower limit (10–11 m), *Pterosiphonia complanata* dominated, occasionally accompanied by patches of *G. corneum* (Gorostiaga, 1995). By 2007, the gradual increase in SST, exacerbated by temperature peaks in 2003 and 2006, led to notable changes in the community at depths of 3–9 m, primarily marked by the decline of *G. corneum*. In contrast, the original turf algal vegetation at 2 m showed fewer evident changes, as the species adapted to these depths were better suited to higher temperature conditions. By 2020, communities at 6 and 9 m had become more akin to the shallow (2 and 3 m) than to the deep (10 and 11 m) communities. The newly established substitute vegetation for the original *G. corneum* stands consisted mainly of coralline species (*Corallina* spp., *Jania rubens*) with patches of *Halopithys incurva* and *Codium decorticatum*. This phenomenon of vegetation change, gradually advancing from shallower to deeper depths, underscores the amplified effects of warming in shallower depths. It further illustrates that the impacts propagate deeper in the water column in a sustained warming scenario, mirroring the patterns observed in thermal requirements. CTI values at 6 and 9 m increased, approaching those of shallow communities, indicating a relative increase of warm-affinity species at these depths. Conversely, at 10 and 11 m, CTI values remained relatively stable at around 12 °C throughout the study period, with a slight dip in 2020 (11.80 °C) compared to 1982 (11.97 °C). An exception was the CTI increase recorded at 11 m depth in 2007, primarily driven by an increase in *Codium decorticatum* and a decrease in *Calliblepharis ciliata* and *Heterosiphonia plumosa* (Appendix H). Although changes in deeper vegetation (10–11 m) were less pronounced than in shallow waters, a gradual transformation between 1982 and 2020 was evident in the nMDS. Notably, this period witnessed a general decrease in *G. corneum*, *P. complanata*, *Dictyopteris polypodioides*, and *C. ciliata* accompanied by an increase in *Gongolaria baccata*. This *G. baccata*-dominated community presented a complex structure, increasing species richness, from 37 in 1982 to around 50 in 2020. This species can grow up to 1 m and foster a complex structure supporting numerous associated species (García-Fernández and Bárbara, 2016). The

proliferation of *G. baccata* did not occur at shallower depths, except for one single quadrat with a high biomass of *G. baccata* at a depth of 3 m. This species is less tolerant to high hydrodynamic conditions and can only compete with *G. corneum* under semi-exposed conditions (Gorostiaga et al., 1998). CTI values in deep waters (10–11 m) in 2020 were slightly lower than those in 1982 due to the increase of the canopy-forming *Gongolaria baccata* and the recovery of cold-affinity species such as *H. plumosa* and *P. complanata* in the last period (2014–2020).

Under an overall trend of rising water temperatures in the study area, a contrasting trend emerged in the most recent period (2014–2020), providing an opportunity to study the short-term (six years) community response. At shallow depths, detropicalization was the primary process responsible for the decrease in CTI during this period. We observed a sharp decline in warm-affinity species, particularly *Codium decorticatum*. Absent in 1982, this species reached a high biomass in 2014, primarily at depths of 2 and 3 m. In 2020, it remained present but biomass had diminished, likely due to the increasing distance of SST from its thermal optimum (Appendix H; 18.16 °C) in the years following the temperature peak in 2014. A similar pattern unfolded for other small warm-affinity species, like *Aphanocladia stichidiosa* or *Cladophora lehmanniana*, which took advantage of the SST increase in 2014 to proliferate and subsequently experienced gradual declines. In deep communities within the same period, the predominant process responsible for the CTI decline was borealization, driven by an increase in the canopy-forming *Gongolaria baccata* and other cold-affinity species such as *Heterosiphonia plumosa* and *Pterosiphonia complanata*.

These changes were not attributable to using SST instead of actual temperature data at different depths to calculate Species Temperature Index (STI). Firstly, the depth-associated temperature variation was minor compared to the broader thermal fluctuations experienced by species globally. The mean thermal range for all algal species in our study (17 °C) was about three times greater than the maximum summer range temperature between 2 and 11 m in our study area (6 °C, personal observation). Secondly, our methodology ensured a consistent calculation of thermal traits across depth and time, with CTI changes driven by shifts in algal abundance rather than computational factors. In fact, we observed differences in composition and thermal traits at equal depths, mitigating biases associated with variations in thermal traits calculated using SST while algae inhabit multiple depths.

Interestingly, temperature alone did not appear to drive changes in deep community structure, as evidenced by consistently low CTI values. The species *G. corneum* failed to recover at these depths. While some studies have reported the migration of certain macroalgal species to higher depths as an adaptation to global warming (Pehlke and Bartsch, 2008; Voerman et al., 2013), it is essential to consider species-specific environmental requirements beyond temperature, such as light availability or wave exposure (Eriksson and Bergström, 2005; Markager and Sand Jensen, 1992). Increasing irradiance and reduced summer rainfall, leading to enhanced water transparency in the study area (Díez et al., 2012), may have also influenced the growth of this macrophyte, originally adapted to moderate-low irradiance conditions (Quintano et al., 2019; Sainz-Villegas et al., 2023).

Community-based metrics are becoming of great importance to understanding the ongoing transformations within global change scenarios. Canopy-forming species are progressively giving way to morphologically simpler species of warmer affinity, such as turfs and coralline species. This shift results in a loss of three-dimensionality and associated ecosystem services. We found a significant positive correlation between CTI and SST, yet our observed correlation failed within bootstrap-generated 95 confidence intervals. We considered both results cautiously, recognizing the limitations of both methods. With a sample size of 6 data points, we could expect a lack of power, making it challenging to detect significant associations. In our study, CTI correlated with SST so that we might see a significant non-existing association (Type I Error). Bootstrapped p-values might still be imprecise with a small sample size, and the method's performance can be limited in detecting genuine associations. The limitations imposed by the small sample size highlight the importance of cautious interpretation, and the need for external validation can help strengthen the reliability of the findings. Ecological theory, observational studies, long-term monitoring, and experimental studies support the positive association between CTI and SST in our study. Using global-scale abundance datasets, Stuart Smith et al. (2015) found a strong correlation between SST and CTI for invertebrate and fish. De Azevedo et al. (2023) concluded that increasing SST with increasing latitude off the Portuguese coast had an evident effect on the CTI of subtidal macroalgal communities. Several studies showed that marine species closely track their thermal tolerances (Poloczanska et al., 2013; Sunday et al., 2012), i.e., increasing temperature will reshape the distribution and abundance of the species and, consequently, alter the CTI.

Global databases have emerged as indispensable tools to address how species migrate in search of optimal survival conditions. This phenomenon is evident in studies spanning diverse regions, from cold-temperate western Australia (Wernberg et al., 2016) to Eastern Canada (Filbee-Dexter et al., 2016) or the Mediterranean Sea (Orlando--Bonaca et al., 2021). The Northern Iberian Peninsula is not an exception, standing as one of the regions most affected by climate change (Belkin, 2009) and with documented distributional shifts of several canopy-forming species (Casado-Amezúa et al., 2019). Our findings agree with other studies in the Iberian Peninsula, along coastal transitional zones. For instance, on the continental Portuguese coast, de Azevedo et al. (2023) reported an increase in CTI in only six years, together with an increase in diversity and biomass. Arriaga et al. (2023) also found a swift community response to rising sea surface temperatures, with CTI increasing over four years in the northern Iberian Peninsula. In both studies, canopy-forming species were being replaced by warm-affinity turf-like species, coinciding with the results of the present study. These studies underscore the role of temperature in explaining the shifts observed in macroalgal communities.

With insights gleaned from species distribution and projections of future warming scenarios, we could anticipate and identify species at risk in specific locations and identify potential climatic refugia. For instance, during a marine heatwave event, Verdura et al. (2021) identified potential climatic refugia for the brown macroalgae *Ericaria crinita* along the Spanish Mediterranean coast. By identifying vulnerable species and their locations, we could take proactive measures to protect those species before irreversible collapse occurs. While we may have limited short-term control over temperature increases, efforts to mitigate other local human stressors such as pollution, fishing, or eutrophication are critical to the health of our oceans (Brown et al., 2013). Sustained long-term monitoring is fundamental to understanding the current state and trends of our benthic communities. Although temperature emerges as the primary driver of distribution changes in the marine realm, local factors such as river influences, upwelling systems, shading cliffs, or intensive recreational activities (such as fishing and diving) can significantly influence communities. Understanding how these communities evolve is paramount to discerning the primary factors responsible for these transformations (Brown et al., 2013; Strain et al., 2014).

The present study covered a time span of 38 years (1982–2020), yet only four years were subject to sampling during this period. At the beginning of the 21st century, two notable SST peaks occurred in 2003 and 2006, marked by particularly scorching summers (Díez et al., 2012). Subsequently, three additional SST peaks occurred in 2011, 2014, and 2020, and their effects have been documented through the data presented in our study. While heatwaves have enormous consequences for benthic communities, the cumulative heat trapped within the oceans also exerts a profound impact, as suggested by the findings of our nearly 40-year-long dataset. Other authors identified shifts in macroalgal communities near our study sites at the turn of the 21st century (Borja et al., 2018; Díez et al., 2012). Considering the destructive nature of the sampling design and the consequent intensive field sampling and laboratory work, our dataset was restricted to seven replicates spanning over two km of the Cantabrian Sea. Despite the limitations of our work, we

believe our study holds considerable value as it can be of use as an early warning system for potential shifts in biological communities in the region. Notably, this study initiated the foundation for more expansive monitoring studies along the Basque Coast (Díez et al., 2003, 2012; Gorostiaga et al., 1998; Muguerza et al., 2017), and unveiled the initial stress symptoms associated with climate change in the area (Muguerza et al., 2022b).

Our study has shed some light on the intricate journey of temperate macroalgal communities in response to increasing sea surface temperatures and varying depths. The observed trends undeniably supported climate-induced changes, with a pronounced impact on these essential underwater ecosystems. The progressive decline in cold-affinity species and the rise of warm-affinity counterparts at shallower depths illustrated the profound influence of temperature on these communities. The exceptional warmth of 2014 and subsequent cooler years highlighted the high sensitivity macroalgae showed to even short-term climate fluctuations. The consequences of these shifts are substantial. Canopy-forming species are being progressively replaced by simpler, warmer-affinity species, resulting in a loss of three-dimensional structure and associated ecosystem services.

Moreover, our study also emphasized the global nature of this problem, with similar shifts documented in diverse regions worldwide (Filbee-Dexter and Wernberg, 2018; Orlando-Bonaca et al., 2021; Steneck et al., 2002; Tanaka et al., 2012). We must recognize the urgency of this issue and take proactive measures to protect vulnerable species and their habitats. While temperature emerges as the primary driver of change, other important local and global factors exist. We may not have immediate control over rising temperatures, but addressing other human stressors such as pollution, overfishing, and eutrophication is within our grasp and is essential to preserving the health of our oceans. Locations under the influence of local factors such as upwellings, rivers, or shaded cliffs may help mitigate the effect of rising temperatures in the regions and function as refugia. Understanding the complex interplay of these factors is crucial for deciphering the dynamics of these transformations (Helmuth et al., 2006; Verdura et al., 2021). Our study served as an early warning system for potential shifts in biological communities in our region and as a model for broader monitoring initiatives (Muguerza et al., 2022a). The limitations of our work also underscored the urgent need for sustained, long-term monitoring efforts at local, regional, national, and international levels to comprehensively understand and address the ongoing transformations in temperate macroalgal communities. We stand at a critical juncture where science, conservation, and policy must unite to protect these invaluable ecosystems and mitigate the global degradation we have contributed to through climate change and other human activities.

CRediT authorship contribution statement

O. Arriaga: Writing – review & editing, Writing – original draft, Visualization, Methodology, Investigation, Formal analysis, Data curation, Conceptualization. **P. Wawrzynkowski:** Visualization, Software, Data curation. **N. Muguerza:** Writing – review & editing, Supervision, Investigation. **I. Díez:** Writing – review & editing, Supervision, Investigation. **J.M. Gorostiaga:** Writing – review & editing, Supervision, Resources, Investigation, Conceptualization. **E. Quintano:** Writing – review & editing, Supervision, Investigation. **M.A. Becerro:** Writing – review & editing, Supervision, Methodology, Formal analysis, Conceptualization.

Declaration of competing interest

The authors declare that they have no known competing financial interests or personal relationships that could have appeared to influence the work reported in this paper.

Data availability

Data will be made available on request.

Acknowledgements

This work was supported by the DIVERSAT project (Spanish Ministry of Science RTI2018-098970-B-I00) and Basque Goverment for the predoctoral grant.

The main author is financially supported by a Basque Government predoctoral grant (Reference No: PRE_2022_2_0127)

Appendix A. Summary of PERMDISP results testing for the effects of Year on 1) CTI, 2) Biomass, 3) Shannon diversity and 4) Species richness. Pairwise comparisons are also shown

1) PERMDISP-CTI			
F	**Df1**	**Df2**	**p**
14.507	3	132	0.0001
Pairwise comparison between years			
	1982≠2007	2007 = 2014	
	1982≠2014	2007 = 2020	
	1982≠2020	2014≠2020	
2) PERMDISP- Biomass			
F	**Df1**	**Df2**	**p**
2.9252	3	132	0.1394
Pairwise comparison between years			
	1982≠2007	2007 = 2014	
	1982 = 2014	2007 = 2020	
	1982 = 2020	2014 = 2020	
3) PERMDISP- Shannon			
F	**Df1**	**Df2**	**p**
3.3566	3	132	0.0234
Pairwise comparison between years			
	1982 = 2007	2007 = 2014	
	1982≠2014	2007 = 2020	

(*continued on next page*)

(*continued*)

3) PERMDISP- Shannon			
	1982≠2020	2014 = 2020	
4) PERMDISP- Species richness			
F	**Df1**	**Df2**	**p**
4.2542	3	132	0.0073
Pairwise comparison between years			
	1982≠2007	2007≠2014	
	1982 = 2014	2007≠2020	
	1982 = 2020	2014 = 2020	

Appendix B. Summary of PERMANOVA results testing for the effects of Year, Depth, and the interaction of the two factors on 1) CTI, 2) Biomass, 3) Shannon diversity and 4) Species richness. Pairwise comparisons for significant test are also shown

1) PERMANOVA-CTI						
	df	SS	MS	Pseudo-F	p	
Year	3	27.625	9.2083	6.015	0.0008	
Depth	5	102.6	20.521	6.6988	0.0019	
Year X Depth	15	46.197	3.0798	2.0118	0.021	
Res	112	171.46	1.5309			
Total	135	367.68				
Pairwise comparisons between years for each depth						
	2 m	3 m	6 m	9 m	10 m	11 m
	1982 = 2007	1982≠2007	1982 = 2007	1982 = 2007	1982 = 2007	1982 = 2007
	1982 = 2014	1982≠2014	1982 = 2014	1982 = 2014	1982 = 2014	1982 = 2014
	1982≠2020	1982≠2020	1982≠2020	1982≠2020	1982 = 2020	1982 = 2020
	2007 = 2014	2007 = 2014	2007 = 2014	2007 = 2014	2007 = 2014	2007 = 2014
	2007 = 2020	2007 = 2020	2007≠2020	2007 = 2020	2007 = 2020	2007 = 2020
	2014 = 2020	2014 = 2020	2014 = 2020	2014 = 2020	2014 = 2020	2014 = 2020
Pairwise comparisons between depths for each year						
1982	2≠3	2≠6	2≠9	2≠10	2≠11	3 = 6
	3 = 9	3≠10	3≠11	6 = 9	6 = 10	6≠11
	9 = 10	9 = 11	10 = 11			
2007	2 = 3	2 = 6	2 = 9	2≠10	2 = 11	3 = 6
	3 = 9	3≠10	3 = 11	6 = 9	6 = 10	6 = 11
	9 = 10	9 = 11	10 = 11			
2014	2 = 3	2 = 6	2≠9	2≠10	2≠11	3 = 6
	3≠9	3≠10	3≠11	6 = 9	6 = 10	6≠11
	9 = 10	9≠11	10 = 11			
2020	2 = 3	2 = 6	2 = 9	2≠10	2≠11	3 = 6
	3 = 9	3≠10	3≠11	6 = 9	6≠10	6≠11
	9≠10	9≠11	10 = 11			
2) PERMANOVA-Biomass						
	df	**SS**	**MS**	**Pseudo-F**	**p**	
Year	3	15131	5043.7	1.105	0.3529	
Depth	5	56815	11363	1.6505	0.2056	
Year X Depth	15	1.0365E5	6909.7	1.5138	0.1104	
Res	112	5.1122E5	4564.4			
Total	135	6.9966E5				
3) PERMANOVA-Shannon						
	df	SS	MS	Pseudo-F	p	
Year	3	18.606	6.2021	8.2231	0.0001	
Depth	5	14.337	2.8675	2.861	0.0554	
Year X Depth	15	15.074	1.0049	1.3324	0.1929	
Res	112	84.474	0.75423			
Total	135	134.57				
Pairwise comparison for factor Year						
	1982 = 2007	2007 = 2014				
	1982≠2014	2007≠2020				
	1982≠2020	2014 = 2020				
4) PERMANOVA-Species richness						
	df	SS	MS	Pseudo-F	p	

(*continued on next page*)

(*continued*)

4) PERMANOVA-Species richness					
	df	SS	MS	Pseudo-F	p
Year	3	7367.3	2455.8	15.464	0.0001
Depth	5	1043.4	208.68	2.0463	0.1418
Year X Depth	15	1520.5	101.37	0.63831	0.8359
Res	112	17786	158.8		
Total	135	27854			
Pairwise comparison for factor Year					
	1982≠2007	2007≠2014			
	1982 = 2014	2007≠2020			
	1982≠2020	2014≠2020			

Appendix C. Average biomass (g DW · 2000 cm^{-2}) and contribution (%) of the taxa to the dissimilarity between 1982 and 2020 according to the SIMPER routine. Only taxa with a contribution >1% to the average dissimilarity are included.[1] Ellisolandia elongata and Corallina officinalis, [2] Xiphosiphonia ardreana and Xiphosiphonia pennata. Blue shading: taxa forming decrease group. Orange shading: taxa forming increase group

SIMPER results			
Groups 1982 & 2020: Average dissimilarity = 86,45			
Species	**Av. biomass 1982**	**Av. biomass 2020**	**Contribution (%)**
Gelidium corneum	89.569	27.223	22.34
Gongolaria baccata	0	28.408	6.76
Corallina spp.[1]	0.278	5.963	5.62
Jania rubens	0.055	5.584	5.13
Pterosiphonia complanata	4.691	2.683	4.91
Halopithys incurva	2.443	7.547	4.73
Asparagopsis armata	1.902	0.008	3.06
Dictyopteris polypodioides	1.932	0.343	2.85
Peyssonnelia squamaria	0.003	1.371	2.26
Heterosiphonia plumosa	0.893	0.863	2.20
Calliblepharis ciliata	1.609	0	2.06
Phyllophora crispa	0	1.252	2.02
Codium fragile	0	2.391	1.99
Plocamium cartilagineum	0.587	0.904	1.96
Xiphosiphonia spp.[2]	0.155	0.859	1.75
Codium decorticatum	0	3.332	1.69
Cryptopleura ramosa	0.173	0.802	1.65
Taonia atomaria	0	0.657	1.52
Gelidium spinosum	0.330	0.350	1.50
Dictyota dichotoma	0.221	0.584	1.48
Halopteris scoparia	0.043	0.472	1.40
Halurus equisetifolius	0.033	0.407	1.23
Acrosorium ciliolatum	0.051	0.347	1.19
Codium sp.	0	0.762	1.14
Halopteris filicina	0.096	0.303	1.13
Sphaerococcus coronopifolius	0	1.035	1.06

Appendix D. Summary of PERMANOVA results testing for the effects of Year, Group, and the interaction of the two factors on the Biomass. Pairwise comparisons for significant test are also shown at the bottom

PERMANOVA-Biomass groups					
	df	SS	MS	Pseudo-F	p
Year	3	15545	5181.7	1.8464	0.1386
Group	1	5004.9	5004.9	5.7418 E−2	0.8302
Year X Group	3	2.6186 E5	87288	31.104	0.0001
Res	264	7.4087 E5	2806.3		
Total	271	1.0259 E6			

Pairwise comparisons between years for each group		Pairwise comparisons between groups for each year	
Increase	Decrease		
1982≠2007	1982≠2007	1982	Increase ≠ Decrease
1982≠2014	1982≠2014	2007	Increase = Decrease
1982≠2020	1982≠2020	2014	Increase ≠ Decrease
2007 = 2014	2007≠2014	2020	Increase ≠ Decrease

(*continued on next page*)

(*continued*)

Pairwise comparisons between years for each group		Pairwise comparisons between groups for each year
Increase	Decrease	
2007 = 2020	2007≠2020	
2014 = 2020	2014 = 2020	

Appendix E. Single factor analysis of variance (ANOVA) for CTI (ºC) of groups (increase, decrease)

Groups	Count	Sum	Average	Variance
Increase	20	272.356	13.618	4.366
Decrease	6	70.156	11.693	2.148

ANOVA

Source of variation	SS	df	MS	F	p-value	F crit
Between groups	17.106	1	17.106	4.382	0.047	4.260
Within groups	93.699	24	3.904			
Total	110.806	25				

Appendix F. Summary of PERMDISP results testing for the effects of Year on the community structure. Pairwise comparisons are also shown

PERMDISP-Community structure			
F	**Df1**	**Df2**	**p**
6.1	3	132	0.0012
Pairwise comparison between years			
	1982≠2007	2007 = 2014	
	1982≠2014	2007 = 2020	
	1982≠2020	2014 = 2020	

Appendix G. Summary of PERMANOVA results testing for the effects of Year, Depth, and the interaction of the two factors on the community structure. Pairwise comparisons for significant test are also shown

PERMANOVA-Community structure						
	df	**SS**	**MS**	**Pseudo-F**	**p**	**Unique perms**
Year	3	80336	26779	12.549	0.0001	9887
Depth	5	62207	12441	3.8329	0.0001	9929
Year X Depth	15	48869	3257.9	1.5267	0.0004	9756
Res	112	2.39 E5	2133.9			
Total	135	4.4208 E5				
Pairwise comparisons between years for each depth						
	2m	**3m**	**6m**	**9m**	**10m**	**11m**
	1982 = 2007	1982≠2007	1982≠2007	1982 = 2007	1982≠2007	1982≠2007
	1982≠2014	1982≠2014	1982≠2014	1982≠2014	1982≠2014	1982≠2014
	1982≠2020	1982≠2020	1982≠2020	1982≠2020	1982≠2020	1982≠2020
	2007≠2014	2007≠2014	2007≠2014	2007 = 2014	2007 = 2014	2007 = 2014
	2007≠2020	2007≠2020	2007≠2020	2007≠2020	2007 = 2020	2007 = 2020
	2014≠2020	2014≠2020	2014≠2020	2014 = 2020	2014≠2020	2014 = 2020
Pairwise comparisons between depths for each year						
1982	2≠3	2≠6	2 = 9	2 = 10	2≠11	3 = 6
	3≠9	3≠10	3≠11	6 = 9	6≠10	6≠11
	9 = 10	9 = 11	10 = 11			
2007	2 = 3	2≠6	2 = 9	2≠10	2≠11	3 = 6
	3 = 9	3≠10	3≠11	6 = 9	6≠10	6≠11
	9 = 10	9 = 11	10 = 11			
2014	2 = 3	2 = 6	2≠9	2≠10	2≠11	3 = 6
	3 = 9	3≠10	3≠11	6 = 9	6 = 10	6 = 11
	9 = 10	9 = 11	10 = 11			
2020	2 = 3	2≠6	2≠9	2≠10	2≠11	3 = 6
	3≠9	3≠10	3≠11	6 = 9	6≠10	6≠11
	9 = 10	9≠11	10 = 11			

Appendix H. Thermal optimum (TO) and average biomass of the main taxa for each depth and year.[1] Ellisolandia elongata and Corallina officinalis

Taxa		2 m				3 m				6 m				9 m				10 m				11 m			
	TO	1982	2007	2014	2020	1982	2007	2014	2020	1982	2007	2014	2020	1982	2007	2014	2020	1982	2007	2014	2020	1982	2007	2014	2020
Gelidium corneum	12.48	10.48	13.58	0.04	0.98	189.4	49.94	1.64	3.89	149.5	72.70	13.37	5.50	63.74	14.05	0.40	0.96	43.67	0.10	0.48	0.31	0.25	0.15	0.01	0.02
Gongolaria baccata	11.54	–	0.06	0.46	–	–	–	–	41.03	–	9.44	25.19	0.67	–	21.84	28.15	1.67	–	60.63	33.45	57.39	–	27.07	66.73	73.72
Halopithys incurva	13.00	18.66	29.68	45.24	13.90	–	16.15	20.85	16.46	0.27	–	0.01	2.20	0.02	1.70	1.20	4.93	0.21	7.54	0.79	0.50	0.20	–	1.22	0.01
Corallina spp.[1]	15.36	1.36	5.99	1.34	12.0	0.27	1.41	5.01	8.58	0.17	0.25	0.74	2.82	0.09	0.67	3.79	3.60	–	0.09	3.95	3.57	–	–	0.03	0.04
Jania rubens	15.59	0.10	0.28	2.62	14.03	–	2.03	9.38	10.64	–	0.02	0.23	1.78	0.08	0.70	0.24	0.49	0.17	0.33	0.13	0.32	–	0.17	0.10	0.03
Pterosiphonia complanata	11.97	2.28	0.22	0.03	0.08	0.77	0.03	0.06	0.31	1.59	0.06	0.08	1.09	3.92	0.65	0.54	5.23	14.67	0.58	0.35	6.08	7.31	0.39	1.41	4.71
Codium decorticatum	18.16	–	24.66	16.87	0.14	–	10.61	45.68	–	–	0.23	5.23	0.21	–	0.20	3.20	21.63	–	0.02	0.18	–	–	2.75	–	–
Calliblepharis ciliata	10.44	–	–	–	–	0.18	–	–	–	0.01	–	0.30	–	1.84	0.21	–	–	3.79	0.01	0.06	–	5.04	0.13	0.60	–
Heterosiphonia plumosa	9.58	0.11	–	–	–	–	–	0.01	–	0.01	–	0.16	–	0.59	0.12	0.07	0.19	0.97	0.02	0.26	0.91	4.92	0.07	0.25	5.51
Phyllophora crispa	10.08	–	0.03	–	0.17	–	0.04	–	0.04	–	0.06	0.67	1.35	–	0.72	0.63	0.80	0	0.42	13.22	1.50	–	4.99	4.55	5.36

References

Anderson, M.J., Gorley, R.N., Clarke, K.R., 2008. PERMANOVA+ for PRIMER: Guide to Software and Statistical Methods. PRIMER-E", Plymouth, UK.

Arriaga, O., Wawrzynkowski, P., Ibáñez, H., Muguerza, N., Díez, I., Pérez-Ruzafa, I., Gorostiaga, J.M., Quintano, E., Becerro, M.A., 2023. Short-term response of macroalgal communities to ocean warming in the Southern Bay of Biscay. Mar. Environ. Res. 190, 106098 https://doi.org/10.1016/j.marenvres.2023.106098.

Assis, J., Berecibar, E., Claro, B., Alberto, F., Reed, D., Raimondi, P., Serrão, E.A., 2017. Major shifts at the range edge of marine forests: the combined effects of climate changes and limited dispersal. Sci. Rep. 7, 44348 https://doi.org/10.1038/srep44348.

Belkin, I.M., 2009. Rapid warming of large marine ecosystems. Prog. Oceanogr. 81, 207–213. https://doi.org/10.1016/j.pocean.2009.04.011.

Borja, A., Aguirrezabalaga, F., Martínez, J., Sola, J.C., García-Arberas, L., Gorostiaga, J. M., 2004. Benthic communities, biogeography and resources management. In: Borja, A., Collins, M. (Eds.), Oceanography and Marine Environment of the Basque Country, vol. 70. Elsevier Oceanography Series, pp. 455–492. https://doi.org/10.1016/S0422-9894(04)80056-4.

Borja, A., Chust, G., Fontán, A., Garmendia, J.M., Uyarra, M.C., 2018. Long-term decline of the canopy-forming algae *Gelidium corneum*, associated to extreme wave events and reduced sunlight hours, in the southeastern Bay of Biscay. Estuarine. Coast. Shelf Sci. 205, 152–160. https://doi.org/10.1016/j.ecss.2018.03.016.

Borja, Á., Egaña, J., Valencia, V., Franco, J., Castro, R., 2000. Estudio y validación de una serie de datos diarios de temperatura del agua del mar en San Sebastián, procedente de su Aquarium, 1947-1997 Ozeanografika 3, 139–152.

Brown, C.J., Sauders, M.I., Possingham, H.P., Richardson, A.J., 2013. Managing for interactions between local and global stressors of ecosystems. PLoS One 8, e65765. https://doi.org/10.1371/journal.pone.0065765.

Burrows, M.T., Bates, A.E., Costello, M.J., Edwards, M., Edgar, G.J., Fox, C.J., Halpern, B. S., Hiddink, J.G., Pinsky, M.L., Batt, R.D., García Molinos, J., Payne, B.L., Schoeman, D.S., Stuart-Smith, R.D., Poloczanska, E.S., 2019. Ocean community warming responses explained by thermal affinities and temperature gradients. Nat. Clim. Change 9, 959–963. https://doi.org/10.1038/s41558-019-0631-5.

Bustamante, M., Tajadura, J., Gorostiaga, J.M., Saiz-Salinas, J.I., 2014. Response of rocky invertebrate diversity, structure and function to the vertical layering of vegetation. Estuar. Coast Shelf Sci. 147, 148–155. https://doi.org/10.1016/j.ecss.2014.06.001.

Casado-Amezúa, P., Araújo, R., Bárbara, I., Bermejo, R., Borja, Á., Díez, I., Fernández, C., Gorostiaga, J.M., Guinda, X., Hernández, I., Juanes, J.A., Peña, V., Peteiro, C., Puente, A., Quintana, I., Tuya, F., Viejo, R.M., Altamirano, M., Gallardo, T., Martínez, B., 2019. Distributional shifts of canopy-forming seaweeds from the Atlantic coast of Southern Europe. Biodivers. Conserv. 28, 1151–1172. https://doi.org/10.1007/s10531-019-01716-9.

Chamberlain, S., Barve, V., Mcglinn, D., Oldoni, D., Desmet, P., Geffert, L., Ram, K., 2021. Rgbif: Interface to the global biodiversity information facility API. https://CRAN.R-project.org/package=rgbif.

Chust, G., González, M., Fontán, A., Revilla, M., Alvarez, P., Santos, M., Cotano, U., Chifflet, M., Borja, A., Muxika, I., Sagarminaga, Y., Caballero, A., de Santiago, I., Epelde, I., Liria, P., Ibaibarriaga, L., Garnier, R., Franco, J., Villarino, E., Irigoien, X., Fernandes-Salvador, J.A., Uriarte, Andrés, Esteban, X., Orue-Echevarria, D., Figueira, T., Uriarte, A., 2022. Climate regime shifts and biodiversity redistribution in the Bay of Biscay. Sci. Total Environ. 803, 149622 https://doi.org/10.1016/j.scitotenv.2021.149622.

de Azevedo, J., Franco, J.N., Vale, C.G., Lemos, F.L.M., Arenas, P., 2023. Rapid tropicalization evidence of subtidal seaweed assemblages along a coastal transitional zone. Sci. Rep. 13, 11720 https://doi.org/10.1038/s41598-023-38514-x.

Devictor, V., Julliard, R., Couvet, D., Jiguet, F., 2008. Birds are tracking climate warming, but not fast enough. Proc. Royal Soc. B 275, 2743–2748. https://doi.org/10.1098/rspb.2008.0878.

Devictor, V., van Swaay, C., Brereton, T., Brotons, L., Chamberlain, D., Heliölä, J., Herrando, S., Julliard, R., Kuussaari, M., Lindström, Å., Reif, J., Roy, D.B., Schweiger, O., Settele, J., Stefanescu, C., Van Strien, A., Van Turnhout, C., Vermouzek, Z., WallisDeVries, M., Wynhoff, I., Jiguet, F., 2012. Differences in the climatic debts of birds and butterflies at a continental scale. Nat. Clim. Change 2, 121–124. https://doi.org/10.1038/nclimate1347.

Díez, I., Muguerza, N., Santolaria, A., Ganzedo, U., Gorostiaga, J.M., 2012. Seaweed assemblage changes in the eastern Cantabrian Sea and their potential relationship to climate change. Estuar. Coast Shelf Sci. 99, 108–120. https://doi.org/10.1016/j.ecss.2011.12.027.

Díez, I., Santolaria, A., Gorostiaga, J.M., 2003. Relationships of environmental factors to the structure and distribution of subtidal seaweed vegetation of the western Basque coast (N. Spain). Estuarine. Coast. Shelf Sci. 56, 1041–1054. https://doi.org/10.1016/S0272-7714(02)00301-3.

Eriksson, B.K., Bergström, L., 2005. Local distribution patterns of macroalgae in relation to environmental variables in the northern Baltic Proper. Estuar. Coast Shelf Sci. 62, 109–117. https://doi.org/10.1016/j.ecss.2004.08.009.

Fernández, C., 2011. The retreat of large brown seaweeds on the north coast of Spain: the case of *Saccorhiza polyschides*. Eur. J. Phycol. 46, 352–360. https://doi.org/10.1080/09670262.2011.617840.

Filbee-Dexter, K., Feehan, C.J., Scheibling, R.E., 2016. Large-scale degradation of a kelp ecosystem in an ocean warming hotspot. Mar. Ecol. Prog. Ser. 543, 141–152. https://doi.org/10.3354/meps11554.

Filbee-Dexter, K., Wernberg, T., 2018. Rise of turfs: a new battlefront for globally declining kelp forests. Bioscience 68 (2), 64–76. https://doi.org/10.1093/biosci/bix147.

García-Fernández, A., Bárbara, I., 2016. Studies of cystoseira assemblages in northern Atlantic Iberia. An. del Jardín Botánico Madr. 73 (1), e035. https://doi.org/10.3989/ajbm.2403.

GBIF.org, 2023. GBIF Home Page. Available from: https://www.gbif.org.

González, M., Uriarte, A., Fontán, A., Mader, J., Gyssels, P., 2004. Marine dynamics. In: Borja, A., Collins, M. (Eds.), Oceanography and Marine Environment of the Basque Country, vol. 70. Elsevier Oceanography Series, pp. 133–157.

Gorman, D., Horta, P., Flores, A.A., Turra, A., Berchez, F.A.D.S., Batista, M.B., Lopes Filho, E.S., Melo, M.S., Ignacio, B.L., Carneiro, I.M., 2020. Decadal losses of canopy-forming algae along the warm temperate coastline of Brazil. Global Change Biol. 26, 1446–1457. https://doi.org/10.1111/gcb.14956.

Gorostiaga, J.M., 1995. Sublittoral seaweed vegetation of a very exposed shore on the Basque Coast (N. Spain). Bot. Mar. 38 https://doi.org/10.1515/botm.1995.38.1-6.9.

Gorostiaga, J.M., Santolaria, A., Secilla, A., Díez, I., 1998. Sublittoral benthic vegetation of eastern Basque coast (N Spain): structure and environmental factors. Bot. Mar. 41, 455–465.

Gouvêa, L.P., Schubert, N., Martins, C.D.L., Sissini, M., Ramlov, F., Rodrigues, E.R. de O., Bastos, E.O., Freire, V.C., Maraschin, M., Carlos Simonassi, J., Varela, D.A., Franco, D., Cassano, V., Fonseca, A.L., Barufi, J.B., Horta, P.A., 2017. Interactive effects of marine heatwaves and eutrophication on the ecophysiology of a widespread and ecologically important macroalga. Limnol. Oceanogr. 62, 2056–2075. https://doi.org/10.1002/lno.10551.

Guiry, M.D., Guiry, G.M., 2023. AlgaeBase. Worldwide Electronic Publication. National University of Ireland, Galway. https://www.algaebase.org. searched on 12 January 2023.

Harley, C.D.G., Anderson, K.M., Demes, K.W., Jorve, J.P., Kordas, R.L., Coyle, T.A., Graham, M.H., 2012. Effects of climate change on global seaweed communities. J. Phycol. 48, 1064–1078. https://doi.org/10.1111/j.1529-8817.2012.01224.x.

Helmuth, B., Mieszkowska, N., Moore, P., Hawkins, S.J., 2006. Living on the edge of two changing worlds: forecasting the responses of rocky intertidal ecosystems to climate change. Annu. Rev. Ecol. Evol. Systemat. 37 (1), 373–404. https://doi.org/10.1146/annurev.ecolsys.37.091305.110149.

IPCC, 2023. AR6 Synthesis Report: Climate Change 2023. Synthesis Report of the IPCC Sixth Assessment Report (AR6): Summary for Policymakers.

Izquierdo, P., Rico, J.M., Taboada, F.G., González-Gil, R., Arrontes, J., 2022. Characterization of marine heatwaves in the Cantabrian Sea, SW bay of Biscay. Estuarine. Coast. Shelf Sci. 274, 107923 https://doi.org/10.1016/j.ecss.2022.107923.

Lavín, A., Valdés, L., Sánchez, F., Abaunza, P., Forest, A., Boucher, J., Lazure, P., Anne Jegou, A.M., 2006. The Bay of Biscay: the encountering of the ocean and the shelf. In: Robinson, A.R., Brink, K.H. (Eds.), The Global Coastal Ocean: Interdisciplinary Regional Studies and Syntheses. Harvard Press, pp. 933–999.

Markager, S., Sand-Jensen, K., 1992. Light requirements and depth zonation of marine macroalgae. Mar. Ecol. Prog. Ser. 88, 83–92. https://doi.org/10.3354/meps088083.

McLean, M., Mouillot, D., Maureaud, A.A., Hattab, T., MacNeil, M.A., Goberville, E., Lindegren, M., Engelhard, G., Pinsky, M., Auber, A., 2021. Disentangling tropicalization and deborealization in marine ecosystems under climate change. Curr. Biol. 31, 4817–4823. https://doi.org/10.1016/j.cub.2021.08.034.

Muguerza, N., Díez, I., Quintano, E., Bustamante, M., Gorostiaga, J.M., 2017. Structural impoverishment of the subtidal vegetation of southeastern Bay of Biscay from 1991 to 2013 in the context of climate change. J. Sea Res. 130, 166–179. https://doi.org/10.1016/j.seares.2017.06.006.

Muguerza, N., Arriaga, O., Díez, I., Becerro, M.A., Quintano, E., Gorostiaga, J.M., 2022a. A spatially-modelled snapshot of future marine macroalgal assemblages in southern Europe: towards a broader Mediterranean region? Mar. Environ. Res. 176, 105592 https://doi.org/10.1016/j.marenvres.2022.105592.

Muguerza, N., Díez, I., Quintano, E., Gorostiaga, J.M., 2022b. Decades of biomass loss in the shallow rocky subtidal vegetation of the southeastern Bay of Biscay. Mar. Biodivers. 52, 28. https://doi.org/10.1007/s12526-022-01268-2.

OBIS, 2023. Ocean Biodiversity Information System. Intergovernmental Oceanographic Commission of UNESCO. www.obis.org.

Oliver, E.C.J., Donat, M.G., Burrows, M.T., Moore, P.J., Smale, D.A., Alexander, L.V., Benthuysen, J.A., Feng, M., Sen Gupta, A., Hobday, A.J., Holbrook, N.J., Perkins-Kirkpatrick, S.E., Scan-nell, H.A., Strauband, S.C., Wernberg, T., 2018. Longer and more frequent marine heatwaves over the past century. Nat. Commun. 9, 1–12. https://doi.org/10.1038/s41467-018-03732-9,2018.

Orlando-Bonaca, M., Pitacco, V., Lipej, L., 2021. Loss of canopy-forming algal richness and coverage in the northern Adriatic Sea. Ecol. Indicat. 125, 107501 https://doi.org/10.1016/j.ecolind.2021.107501.

Pehlke, C., Bartsch, I., 2008. Changes in depth distribution and biomass of sublittoral seaweeds at Helgoland (North Sea) between 1970 and 2005. Clim. Res. 37 (2–3), 135–147. https://doi.org/10.3354/cr00767.

Perkol-Finkel, S., Airoldi, L., 2010. Loss and recovery potential of marine habitats: an experimental study of factors maintaining resilience in subtidal algal forests at the Adriatic Sea. PLoS One 5, e10791. https://doi.org/10.1371/journal.pone.0010791.

Poloczanska, E.S., Brown, C.J., Sydeman, W.J., Kiessling, W., Schoeman, D.S., Moore, P. J., Brander, K., Bruno, J.F., Buckley, L.B., Burrows, M.T., Duarte, C.M., Halpern, B.S., Holding, J., Kappel, C.V., O'Connor, M.I., Pandolfi, J.M., Parmesan, C., Schwing, F., Thompson, S.A., Richardson, A.J., 2013. Global imprint of climate change on marine life. Nat. Clim. Change 3, 919–925. https://doi.org/10.1038/nclimate1958.

Provoost, P., Bosch, S., 2019. "robis: R client to access data from the OBIS API." ocean biogeographic information system. Intergovernmental oceanographic commission of UNESCO. R package version 2.1.8. cran.r-project.org/package=robis. GetrightsandcontentR Development Core Team. 2023. R: A language and environment for statistical computing. R Foundation for Statistical Computing, Vienna, Austria. URL, Available at: https://www.R-project.org/.).

Quintano, E., Celis-Plá, P.S.M., Martínez, B., Díez, N., Muguerza, N., Figueroa, F.L., Gorostiaga, J.M., 2019. Ecophysiological responses of a threatened red alga to increased irradiance in an *in situ* transplant experiment. Mar. Environ. Res. 144, 166–177. https://doi.org/10.1016/j.marenvres.2019.01.008.

Quintano, E., Díez, I., Muguerza, N., Figueroa, F.L., Gorostiaga, J.M., 2017. Bed structure (frond bleaching, density and biomass) of the red alga *Gelidium corneum* under different irradiance levels. J. Sea Res. 130, 180–188. https://doi.org/10.1016/j.seares.2017.02.008.

Rhein, M., Rintoul, S.R., Aoki, S., Campos, E., Chambers, D., Feely, R.A., Gulev, S., Johnson, G.C., Josey, S.A., Kostianoy, A., Mauritzen, C., Roemmich, D., Talley, L.D., Wang, F., 2013. Observations: ocean. In: Stocker, T.F., Qin, D., Plattner, G.-K., Tignor, M., Allen, S.K., Boschung, J., Nauels, A., Xia, Y., Bex, V., Midgley, P.M. (Eds.), Climate Change 2013: the Physical Science Basis. Contribution of Working Group I to the Fifth Assessment Report of the Intergovernmental Panel on Climate Change. Cambridge University Press, Cambridge, United Kingdom and New York, NY, USA.

RStudio Team, 2016. RStudio. Integrated development for R. RStudio, Inc., Boston, MA. http://www.rstudio.com/.

Sainz-Villegas, S., Sánchez-Asträin, B., Puente, A., Juanes, J.A., 2023. Characterization of *Gelidium corneum*'s (Florideophyceae, Rhodophyta) vegetative propagation process under increasing levels of temperature and irradiance. Mar. Environ. Res. 187, 105966 https://doi.org/10.1016/j.marenvres.2023.105966.

Smale, D.A., 2020. Impacts of ocean warming on kelp forest ecosystems. New Phytol. 225 (4), 1447–1454. https://doi.org/10.1111/nph.16107.

Smale, D.A., Wernberg, T., 2013. Extreme climatic event drives range contraction of a habitat-forming species. Proc. Royal Soc. B 280, 20122829. https://doi.org/10.1098/rspb.2012.2829.

Steneck, R.S., Graham, M.H., Bourque, B.J., Corbett, D., Erlandson, J.M., Estes, J.A., Tegner, M.J., 2002. Kelp forest ecosystems: biodiversity, stability, resilience and future. Environ. Conserv. 29, 436–459. https://doi.org/10.1017/S0376892902000322.

Strain, E.M.A., Thomson, R.J., Micheli, F., Mancuso, F.P., Airoldi, L., 2014. Identifying the interacting roles of stressors in driving the global loss of canopy-forming to mat-forming algae in marine ecosystems. Global Change Biol. 20, 3300–3312. https://doi.org/10.1111/gcb.12619.

Stuart-Smith, R.D., Edgar, G.J., Barrett, N.S., Kininmonth, S.J., Bates, A.E., 2015. Thermal biases and vulnerability to warming in the world's marine fauna. Nature 528, 88–92. https://doi.org/10.1038/nature16144.

Sunday, J.M., Bates, A.E., Dulvy, N.K., 2012. Thermal tolerance and the global redistribution of animals. Nat. Clim. Change 2, 686–690. https://doi.org/10.1038/nclimate1539.

Tanaka, K., Taino, S., Haraguchi, H., Prendergast, G., Hiraoka, M., 2012. Warming off southwestern Japan linked to distributional shifts of subtidal canopy-forming seaweeds. Ecol. Evol. 2, 2854–2865. https://doi.org/10.1002/ece3.391.

Valencia, V., Franco, J., Borja, A., Fontán, A., 2004. Hydrography of the southeastern bay of Biscay. In: Borja, A., Collins, M. (Eds.), Oceanography and Marine Environment of the Basque Country, vol. 70. Elsevier Oceanography Series, pp. 159–187. https://doi.org/10.1016/S0422-9894(04)80045-X.

Verdura, J., Santamaría, J., Ballesteros, E., Smale, D., Cefalì, M.E., Golo, R., de Caralt, S., Vergés, A., Cebrian, E., 2021. Local-scale climatic refugia offer sanctuary for a habitat-forming species during a marine heatwave. J. Ecol. 109, 1758–1773. https://doi.org/10.1111/1365-2745.13599.

Voerman, S.E., Llera, E., Rico, J.M., 2013. Climate driven changes in subtidal kelp forest communities in NW Spain. Mar. Environ. Res. 90, 119–127. https://doi.org/10.1016/j.marenvres.2013.06.006.

Wernberg, T., Bennett, S., Babcock, R.C., de Bettignies, T., Cure, K., Depczynski, M., Dufois, F., Fromont, J., Fulton, C.J., Hovey, R.K., Harvey, E.S., Holmes, T.H., Kendrick, G.A., Radford, B., Santana-Garcon, J., Saunders, B.J., Smale, D.A., Thomsen, M.S., Tuckett, C.A., Tuya, F., Vanderklift, M.A., Wilson, S., 2016. Climate-driven regime shift of a temperate marine ecosystem. Science 353, 169–172. https://doi.org/10.1126/science.aad8745.